

Natural ageing clustering under different quenching conditions in an Al-Mg-Si alloy

Zi Yang^{1,*}, Xiaohe Jiang¹, Xingpu Zhang¹, Meng Liu¹, Zeqin Liang², David Leyvraz²,

John Banhart¹

¹Helmholtz-Centre Berlin for Materials and Energy, Hahn-Meitner-Platz 1, 10409 Berlin, Germany

²Novelis R&T Centre, Sierre, Route des Laminoirs 15, 3960 Sierre, Switzerland

*Corresponding: zi.yang@helmholtz-berlin.de

Supplementary material

SA. Details of quenching by ventilator

Fig. S1a shows the setup for ventilator cooling (VC). The samples are placed in a meshed cage during solution heat treatment. To perform cooling the sample cage is taken out of the furnace held at 540 °C and mounted on the stand against blowing air within ~1 s. The height of the stand and the distance to the ventilator are fixed so that every time cooling is conducted the same position relative to the ventilator is taken. Nine samples are quenched in every batch and there are three non-equivalent positions in the cage as illustrated in **Fig. S1b**. The average cooling rates (from 533 °C to 250 °C) measured at the three positions are 27.2 ± 1.3 , 27.4 ± 1.7 , and 27.8 ± 0.8 (in $\text{K}\cdot\text{s}^{-1}$) for 1, 2 and 3 respectively, where the error margins are based on three different experiments. Thus, quenching in this device is well reproducible and the same for all 9 samples.

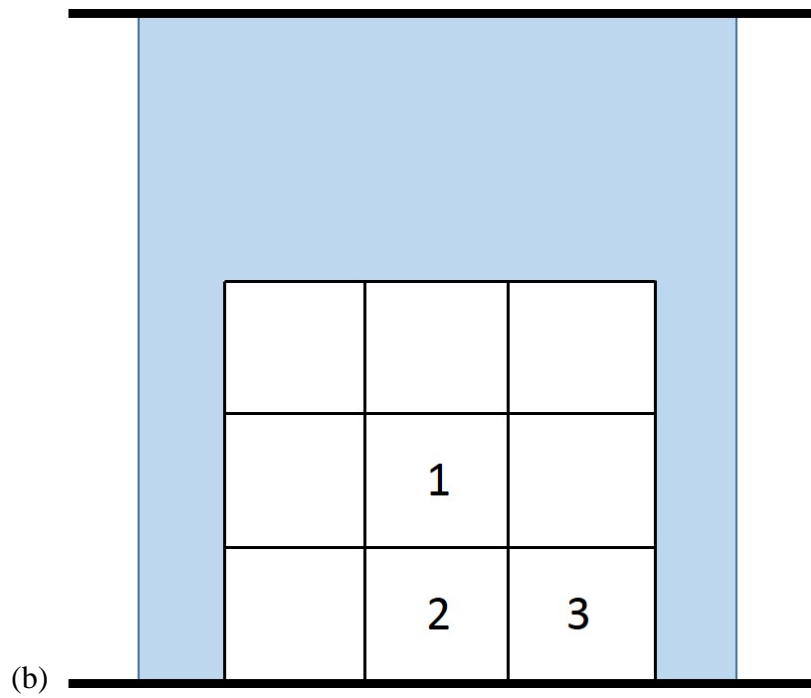
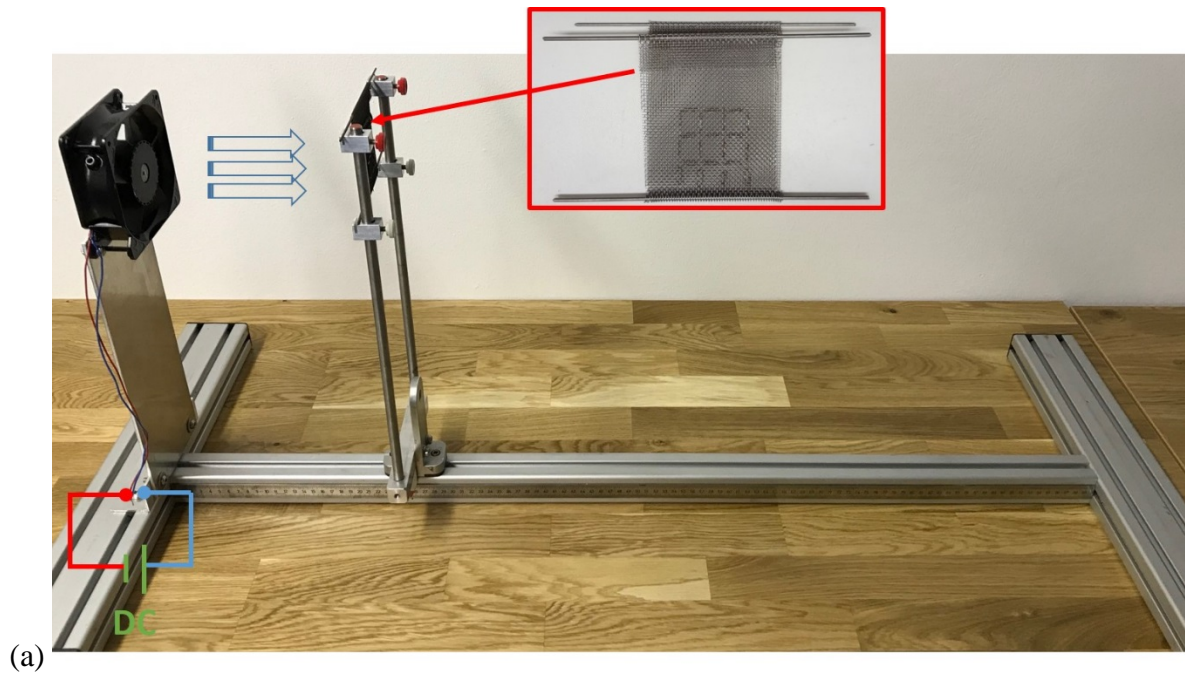


Fig. S1. (a) Cooling setup for ventilator cooling (VC) including the sample cage (in red box). (b) Schematic of the sample cage and the various non-equivalent sample positions: '1' for centre (axis of ventilator), '2' for edge, and '3' for corner.

SB. Positron lifetimes of Al-Mg alloy after Q1-type quenches

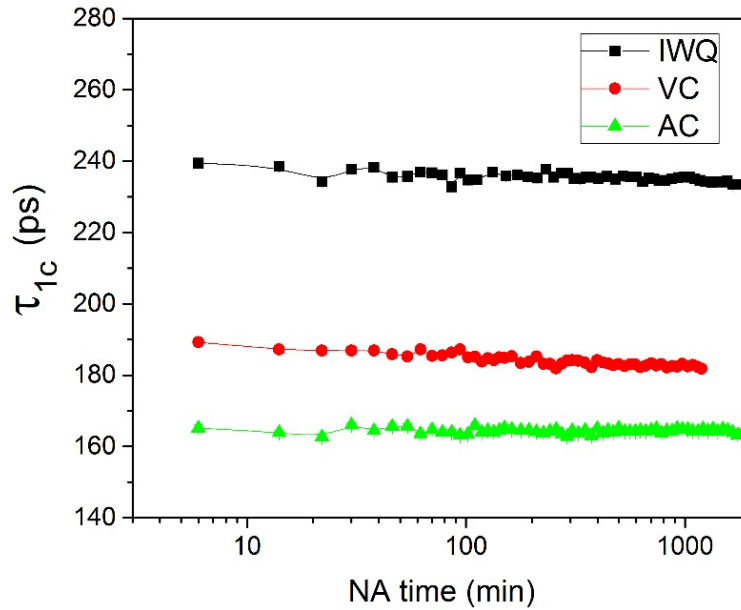


Fig. S2. Positron lifetimes τ_{1c} during NA of binary Al-0.5Mg (wt.%) alloy after various Q1-type quenches.

Fig. S2 displays the positron lifetime evolution in a binary Al-Mg alloy after quenching. It is the analogue to the measurements in Fig. 3. During NA, very little evolution of τ_{1c} is observed. The quenching rate, however, has a pronounced influence on the value of τ_{1c} . After fast quenching, vacancies are efficiently trapped by the Mg atoms, which explains values around 240 ps. During the slowest quenching, in contrast, vacancies can escape from the alloy and a very low value close to 165 ps is observed. This value is similar to that of state AC_200 in Fig. 7b, which was described as a state containing only few vacancies and clusters. Thus, during slow cooling most vacancies are not retained by the Mg atoms and can reach sinks as vacancy-Mg binding is weak well above 'room temperature'.

SC. PALS measurements of Q2-type quenched samples during NA

Fig. S3 shows how positron lifetimes evolve at ‘room temperature’ after slow quenches (VC and AC) from 540 °C that were interrupted at a given temperatures (100 °C to 400 °C) by a fast IWQ to preserve the configuration. Most curves feature an initially low value of τ_{1c} , a subsequent increase and a merger into a curve that is almost the same for all the experiments including those in Fig. 3. The insets show the data used for the extrapolation to zero NA time on a linear time scale.

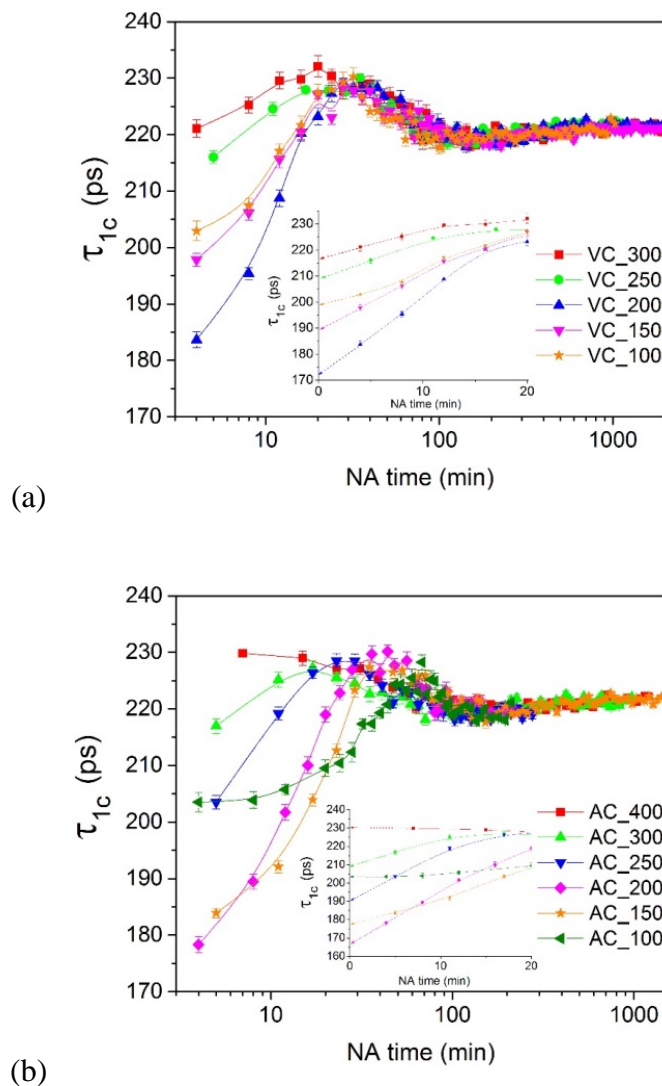


Fig. S3. Positron lifetimes τ_{1c} during NA of samples quenched in a Q2 fashion as shown in Fig. 1 for (a) VC, and (b) AC.

SD. TEM microstructure after various quenching (Q1) and influence on AA hardening

TEM was performed on samples after all three Q1-type quenches (Fig. S4a – c) on a Philips CM30 unit. Observation was conducted in the $\langle 100 \rangle$ directions of the Al matrix. Special attention was paid to secondary particles in the microstructure. Only one type of particle, named P1, can be observed in the microstructure of the IWQ sample, while at least two types of particles, P1 and P2, can be seen for VC and AC. EDX analysis reveals that P1 contains primarily Fe, Si and Mn beside Al, while P2 consists of mainly Mg and Si. P1 particles are observed in many shapes, mostly spherical or ellipsoidal, whereas P2 particles are mostly rod-shaped and are aligned along $\langle 100 \rangle$ directions of the Al matrix. Moreover, P2 particles are mostly attached to P1 or are observed at grain boundaries.

Precipitate formation during VC and AC leads to a reduction of solute supersaturation and consequently to a lower hardening after AA for 30 min or 240 min (peak-age), see Fig. S4d. This is in accordance with previous literature [1]. The formation of clusters during quenching below 200 °C increases hardness in the as-quenched state only marginally (from VC_200 to VC and AC_200 to AC) and has no pronounced influence on AA hardening.

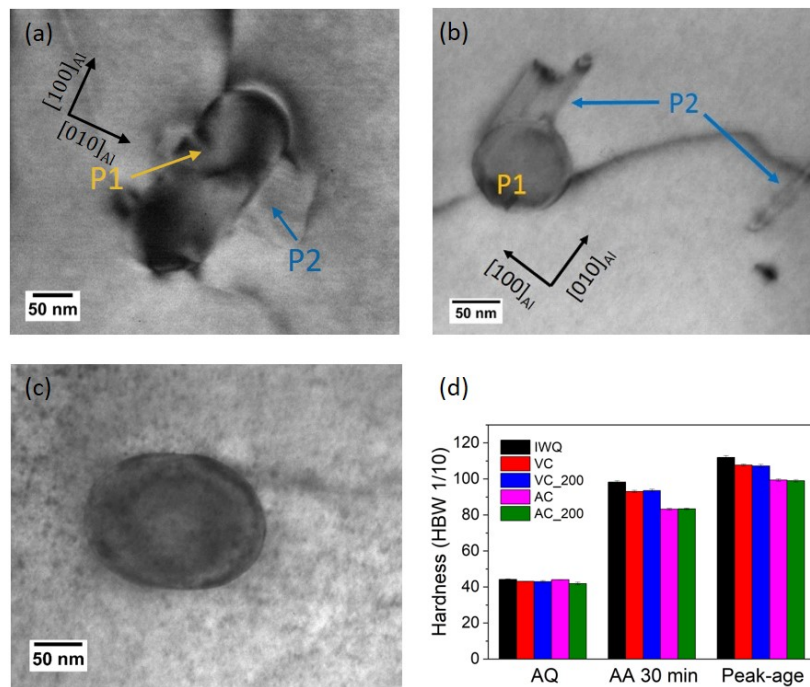


Fig. S4. (a – c) Bright-field TEM images of samples after (a) AC, (b) VC, (c) IWQ. (d) Hardness after various quench routes and subsequent AA conditions. AQ: as-quenched; Peak-age: AA for 240 min.

SE. Vacancy site fraction calculation from positron lifetime

Calculating vacancy fractions from positron lifetime data usually requires decompositions of lifetime spectra into 2 or more components. In this work, we measure τ_{1c} only which, however, is very close to the average positron lifetime that one would calculate from individual components:

$$\tau_{1c} \approx \bar{\tau} = I_0\tau_0 + I_v\tau_v, \quad I_0 + I_v = 1, \quad (1)$$

where the index 0 refers to the reduced bulk lifetime and v to annihilation in vacancy-related defects. $\tau_v = 245$ ps is assumed. By applying the equations of the two-state trapping model [2]:

$$\tau_0 = \frac{1}{\frac{1}{\tau_B} + \kappa_v}, \quad (2)$$

$$I_v = \frac{\kappa_v}{\frac{1}{\tau_B} - \frac{1}{\tau_v} + \kappa_v}, \quad (3)$$

where $\tau_B = 160$ ps is the lifetime in defect-free aluminium, and κ_v is the positron trapping rate of the vacancy-related defect. A relationship applies between κ_v and the site fraction of the vacancies x_v :

$$x_v = \frac{\kappa_v}{\mu}, \quad (4)$$

where μ is the positron trapping coefficient of a vacancy in aluminium. By combining (1 – 4) we eventually obtain the vacancy site fraction

$$x_v = \frac{\tau_B - \bar{\tau}}{\mu\tau_B(\bar{\tau} - \tau_v)}. \quad (5)$$

Using a commonly accepted value $\mu = 250$ ps⁻¹ [3] we can calculate the vacancy site fraction from the one-component positron lifetime. Fig. S5 shows the results, which, however, should not be taken too literally due to the approximations used (e.g. absence of clusters and usage of $\tau_{1c} \approx \bar{\tau}$).

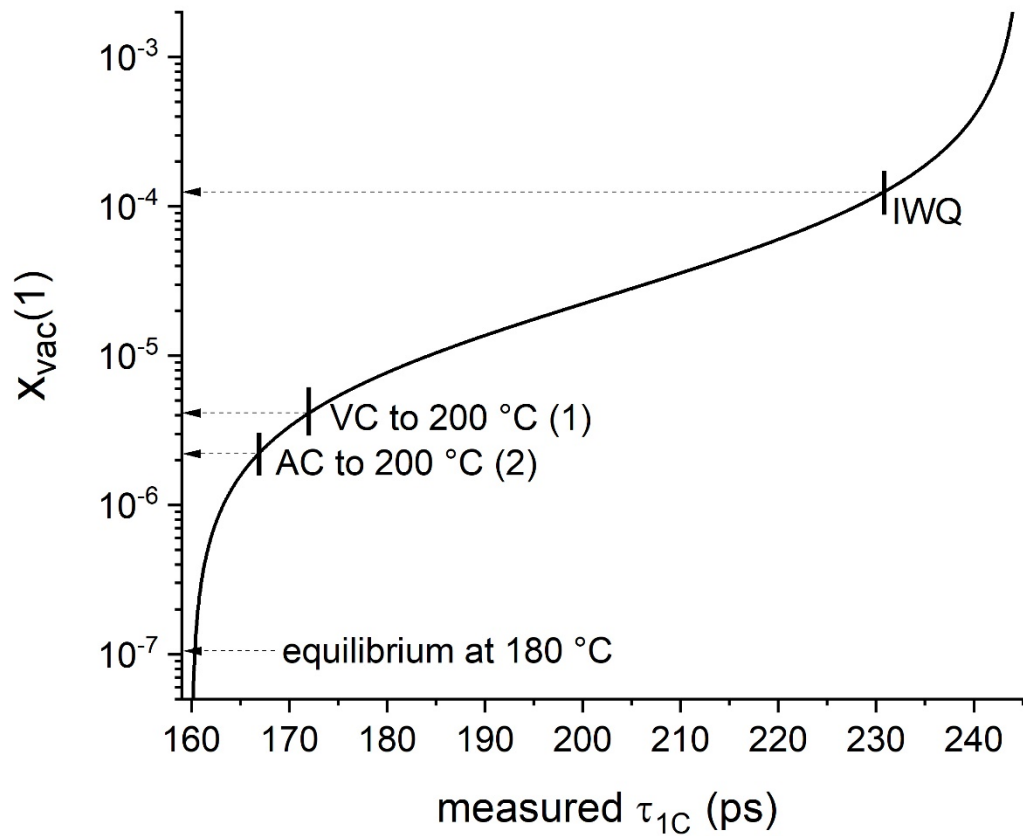


Fig. S5. Vacancy site fraction calculated using Eqs. (1-4) as a function of positron lifetime assuming validity of the positron trapping model for one trap related to vacancies characterised by a lifetime of 245 ps. The upper three arrows correspond to τ_{1C} (extrapolated to zero NA) as measured after three quenches, the lower one marks the equilibrium vacancy fraction at 180 °C as calculated from the formation enthalpy and vibrational entropy of mono-vacancies in Al [4].

References

- [1] B. Milkereit, N. Wanderka, C. Schick, O. Kessler, *Materials Science and Engineering A* 550 (2012) 87-96.
- [2] R. Krause-Rehberg, *Positron Annihilation in Semiconductors*, Springer, Heidelberg, 1999.
- [3] J.A. Jackman, G.M. Hood, R.J. Schultz, *Journal of Physics F: Metal Physics* 17 (1987) 1817.
- [4] T. Hehenkamp, *Journal of Physics and Chemistry of Solids* 55(10) (1994) 907-915.